ACS Macro Letters

pubs.acs.org/macroletters Letter

Conformation of Network Strands in Polymer Gels

Haley K. Beech, Jeremiah A. Johnson, and Bradley D. Olsen*

Cite This: ACS Macro Lett. 2023, 12, 325−330 Read Online

ACCESS | Metrics & More | Article Recommendations | Supporting Information

ABSTRACT: Small angle neutron scattering was used to measure single chain radii of gyration of end-linked polymer gels before and after cross-linking to calculate the prestrain, which is the ratio of the average chain size in a cross-linked network to that of a free chain in solution. The prestrain increased from 1.06 ± 0.01 to 1.16 ± 0.02 as gel synthesis concentration decreased near the overlap concentration, indicating that the chains are slightly more stretched in the network than in solution. Dilute gels with higher loop fractions were found to be spatially homogeneous. Form factor and volumetric scaling analyses independently confirmed that elastic strands stretch by 2−23% from Gaussian conformations to create a space-spanning network, with increased stretching as network synthesis concentration decreases. Prestrain measurements reported here serve as a point of reference for network theories that rely on this parameter for the calculation of mechanical properties.

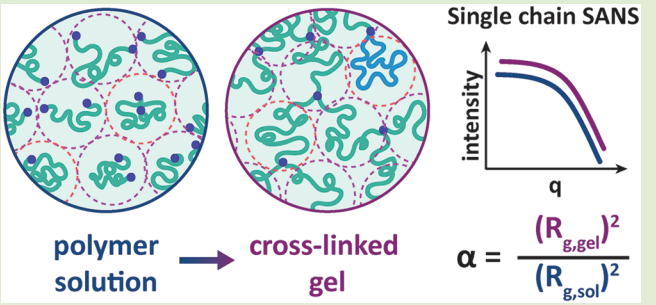

Polymer networks are important materials with an array of applications ranging from common tires[1−3] to biomedical materials such as tissue scaffolds and drug delivery systems.[4−7] Quantitatively predicting the mechanical properties of networks, even the relatively simple linear elasticity, is a long-standing challenge with significant technological importance. This challenge arises because real networks are difficult to accurately characterize due to the formation of defects such as dangling ends and loops which are not fully elastically effective and therefore do not contribute to the mechanical properties of the material to the same extent.[8−12] While recent efforts to incorporate loops into elasticity,[11,13−17] swelling,[18,19] and fracture[20,21] theories have shown improved agreement with experimental data, one uncertainty underlying these updates is the role chain conformation plays in property prediction.

Prestrain represents the change in chain conformations during the cross-linking process, described by the following ratio:

$$\alpha = \frac{\langle R^2 \rangle_0}{Nb^2} \tag{1}$$

where $\langle R^2 \rangle_0$ is the mean square end-to-end distance of strands in the network, N is the number of Kuhn segments, and b is the Kuhn length, assuming a Gaussian conformation in solution. Until recently, most network theories assumed that the average end-to-end distance of a chain was equal before and after gelation.[1,11,22−24] However, loop defects have more compact conformations than free chains in solution; in the case of a primary loop, the end-to-end distance decreases from its Gaussian conformation in solution to zero after the looping reaction. Loops have been shown to become more prevalent as the synthesis concentration decreases, impacting network properties in the semidilute regime.[9−11,25]

Theoretical prestrain differs for strands in loops of different sizes, and these effects contribute significantly to the elasticity of the network.[14,26,27] Lang initially pointed out that elastic modulus predictions vary by a factor of 4, depending on if and how prestrain is incorporated into elasticity theories.[14,15] Lin et al. updated the phantom network-based real elastic network theory to show that a quantitative match between theory and experimental elasticity measurements was achieved only when prestrain of all loops was included.[11,13] Gusev similarly argued that reliable property predictions require a representative 3D network, which can be used to extract key topological factors, including prestrain, to correct a traditional affine or phantom network model.[16] However, neither loop populations larger than second order nor prestrain have been measured experimentally in gels, making various theoretical assumptions difficult to confirm.

Small angle neutron scattering (SANS) has previously been used to measure single chain conformations of both ring polymers and neat networks. SANS is ideally suited for precise substructure measurements using isotope labeling.[28−31] Beltzung et al. measured the radii of gyration of polymer melts and the corresponding end-linked networks in the concentrated regime where loop fractions are expected to be

Received: January 4, 2023
Accepted: February 13, 2023

https://doi.org/10.1021/acsmacrolett.3c00006
ACS Macro Lett. 2023, 12, 325−330

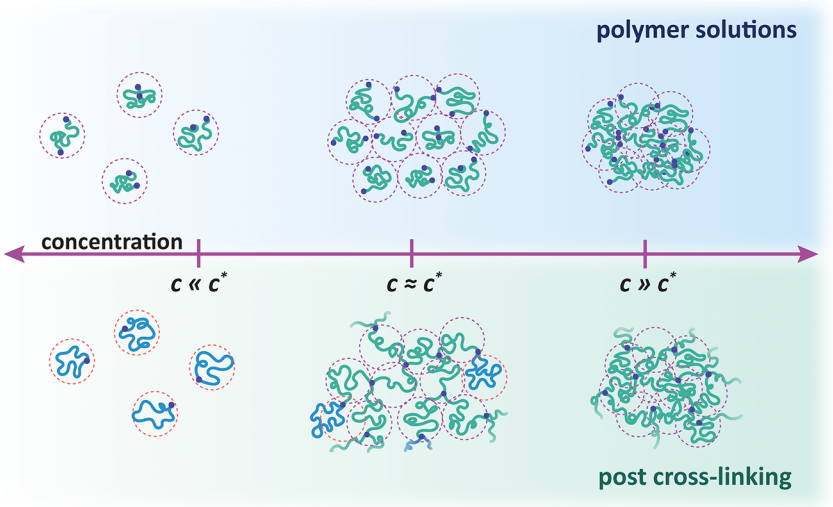

Figure 1. Polymers in the dilute (left), semidilute (center), and concentrated (right) regimes before (top) and after (bottom) cross-linking take on different conformations depending on the concentration, resulting in a wide array of prestrain-dependent properties.

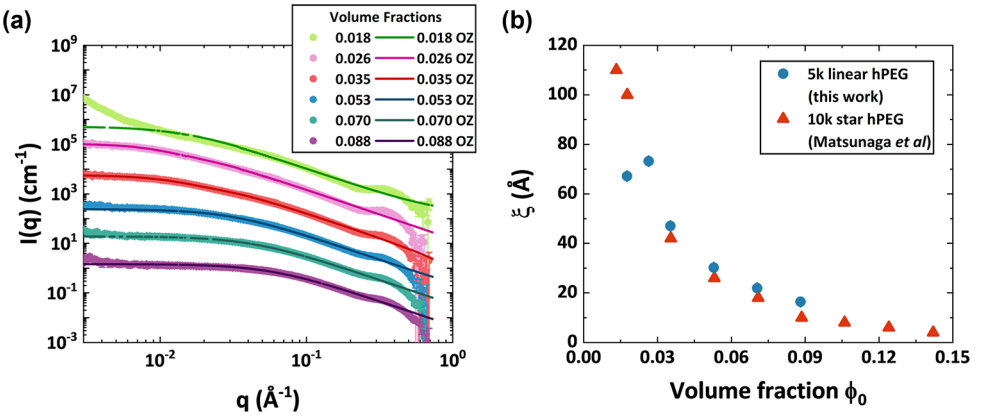

Figure 2. (a) SANS intensity data of hydrogenous PEG gels fit with the Ornstein−Zernike equation. Data were vertically shifted for clarity by multiplicative 10-fold increments for ϕ_0 = 0.070−0.018 data. (b) Correlations lengths for the A_2 + B_4 hPEG networks compared to previously reported correlation lengths of a 10 kDa tetra-PEG network as a function of volume fraction.[42]

negligible.[32] Their results showed no change in the radius of gyration upon cross-linking, providing strong evidence that α = 1 when networks are prepared well above the overlap concentration. Ring polymers have radii of gyration that have been widely confirmed to be approximately half that of the free chain in solution, depending on solvent quality and concentration.[33−37] As shown in Figure 1, these two cases fall on opposite ends of the concentration spectrum. Here, SANS measurements are presented to provide prestrain data in the regime around overlap concentration (center of Figure 1).

To this end, end-linked poly(ethylene glycol) (PEG) gels with primary loop fractions previously quantified via network disassembly spectrometry (NDS) were synthesized and analyzed with SANS.[11] Gels with a mixture of hydrogenous and deuterated chains in deuterated solvent were synthesized at the zero average contrast match (CM) condition to provide single chain information,[30] while pure hydrogenous (hPEG) networks yield information about the overall network. Scattering intensity data for the hPEG networks are plotted as a function of the scattering vector q in Figure 2a. The plateau regions at low q in the hPEG gels show that the gels are relatively homogeneous, even below the overlap polymer volume fraction of $\phi_0^* \approx 0.057$.[38,39] The transition to inhomogeneous scattering at ϕ_0 = 0.018 corresponds to the gel−sol concentration threshold; lower concentration solutions did not form a gel after cross-linking. The bump in the high-q regime corresponds to a length scale on the order of 2−3 Å, a range where features are typically attributed to the amorphous halo generated by short-range order in amorphous polymers.[40] The bump does not influence fitting results, as discussed in the SI.

To quantify these observations, the data were fit to a correlation length model. The Ornstein−Zernike equation captures both inter- and intramolecular thermal concentration fluctuations in networks:[41,42]

$$I(q) = I(0)\left(\frac{1}{1 + q^2\xi^2}\right) + b \tag{2}$$

where $I(0)$ is the low-q intensity plateau, q is the scattering vector, ξ is the correlation length of the network, and b is the incoherent scattering contribution at high-q. Correlation lengths from the A_2 + B_4 hPEG are plotted in Figure 2b and compared to correlation lengths of 10 kDa tetra-arm PEG A_4 +

https://doi.org/10.1021/acsmacrolett.3c00006
ACS Macro Lett. 2023, 12, 325−330

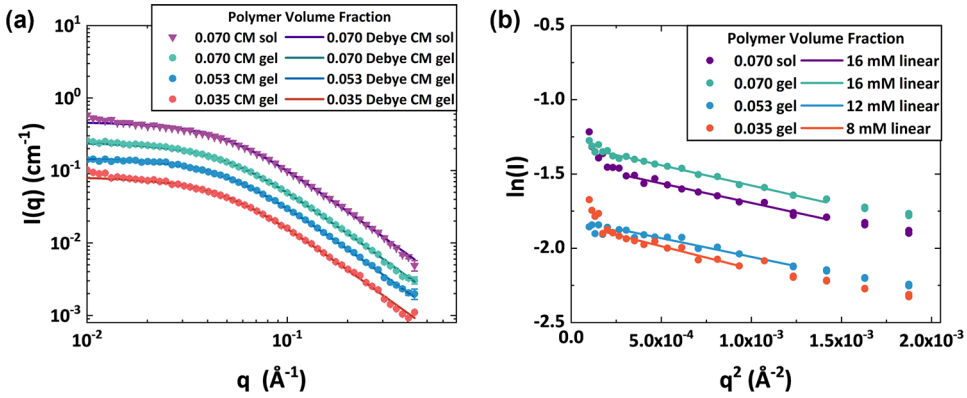

Figure 3. (a) SANS curves for zero average contrast matched PEG gel and solution samples, fit with Debye scattering functions. Data were shifted vertically for clarity by a multiplicative factor of 0.6 for ϕ_0 = 0.035 and 2 for ϕ_0 = 0.070 sol. (b) Guinier plots of ln(I) vs q^2 for the same contrast matched samples, with the slope (drawn as a solid line) equal to $R_g^2/3$.

B_4 networks reported by Matsunaga et al., which have a nearly identical length between cross-links of 5 kDa.[42−44] Although the tetra-PEG A_4 + B_4 chemistry prevents primary loop formation while the gels in this work have primary loop fractions ranging from 0.09 to 0.33, the correlation lengths are in good agreement between the two materials.[43,45−47] This suggests that both of these systems have a similar level of spatial homogeneity, despite known differences in topology. Scaling of correlation length with volume fraction demonstrated a scaling exponent consistent with near-θ solvent conditions, as shown in the Correlation Length Scaling section of the SI.

Single chain measurements, necessary to calculate the prestrain of the network, were generated via Debye fitting and Guinier analysis of the CM SANS data and compared to a prestrain estimate based on primary loop defects. Because SANS yields a measure of chain radius of gyration as opposed to end-to-end distance, prestrain was calculated from the extracted R_g values with a modified prestrain equation:

$$\alpha_{R_g} = \frac{R_{g,\text{network}}^2}{R_{g,\text{solution}}^2} \tag{3}$$

In this work $R_{g,\text{solution}}$ was measured at ϕ_0 = 0.070, which is shown below to be in close agreement with the melt R_g. As the samples were all close to the overlap concentration and near θ conditions, the 16 mM solution sample was taken to be invariant to concentration for the purpose of calculating prestrain.[29,42,48]

Contrast matched SANS data were fit with the Debye function for a Gaussian coil to extract the average radius of gyration, R_g:

$$I(q) = I_0\left(\frac{2\exp(-Z) + Z - 1}{Z^2}\right) + b \tag{4}$$

where $Z = (qR_g)^2$. These fits are shown in Figure 3a, with the R_g values and corresponding prestrain reported in Table 1. The Debye equation assumes θ conditions and a single chain signal, which is supported based on the Correlation Length Scaling and Contrast Matching Analysis detailed in the SI (Figures S3 and S4). An error estimate calculated with the bootstrapping method[49] resulted in similar uncertainties, as reported from the confidence interval of the fit (Figure S5). An alternative method used to extract the radius of gyration is the Guinier approximation:

$$\ln(I) \sim -\frac{q^2R_g^2}{3} \quad \text{where} \quad qR_g < 1 \tag{5}$$

Guinier plots of ln(I) versus q^2 can thus be used to determine the radius of gyration without any assumptions related to the model or solvent quality; plots for the contrast matched gels are shown in Figure 3b, with corresponding R_g values and prestrain values reported in Table 1. The slope of the fit line is sensitive to the exact region used for the fitting, which is reflected in the relatively higher error associated with Guinier versus Debye analysis. All of the Debye R_g values were 1−2 Å greater than the Guinier results, but this bias was consistent across samples such that it resulted in comparable prestrain values. The theoretical radius of gyration for a PEG chain with b = 1.1 nm and m_0 = 137 g/mol[22] is 27.5 Å (see the calculation in SI), in good agreement with the measured solution radius of gyration of 28.7 ± 0.1 Å (Debye) and 28.0 ± 0.6 Å (Guinier) at ϕ_0 = 0.070. Debye prestrain values are greater than one for all concentrations measured and show a slight increase as concentration decreases. The measured values of prestrain are relatively close to Lang's average estimation of α = 1.03 at ϕ_0 = 0.070 and 0.053, deviating as loops become more prevalent at the lower concentration.[14]

The measured prestrain data were compared to estimated prestrain values based on previously reported primary loop fractions and the complementary fraction of bridging strands in Figure 4.[11,12] To compare directly with prestrain from SANS data, an estimated R_g was calculated by weighing the form factors for a Gaussian chain and Gaussian ring by the mole fraction of bridging chains and primary loops, respectively, and

Table 1. Radius of Gyration from Debye and Guinier Analyses with the Corresponding Prestrain Reported at Different Synthesis Concentrations

Synthesis volume fraction	Debye radius of gyration (Å)	Debye prestrain	Guinier radius of gyration (Å)	Guinier prestrain
0.035 gel	30.9 ± 0.2	1.16 ± 0.02	29.9 ± 1.1	1.14 ± 0.06
0.053 gel	29.6 ± 0.1	1.06 ± 0.01	27.5 ± 0.4	0.96 ± 0.04
0.070 gel	29.6 ± 0.1	1.06 ± 0.01	28.6 ± 0.3	1.04 ± 0.03
0.070 solution	28.7 ± 0.1		28.0 ± 0.6	

https://doi.org/10.1021/acsmacrolett.3c00006
ACS Macro Lett. 2023, 12, 325−330

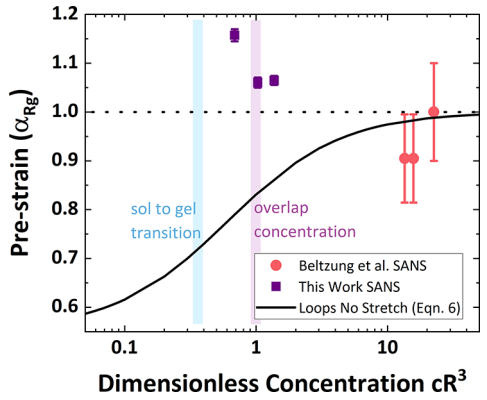

Figure 4. Prestrain as a function of c_{dim} for the gels measured in this work (squares), concentrated PDMS networks measured by Beltzung et al.[32] (circles), and estimated by accounting for primary loops and nonstretching bridging strands (solid line).

setting the sum equal to the form factor used to fit the data as follows:

$$P(R_{g,avg}) = (1 - x_{loop})P(R_{g,bridge}) + (x_{loop})P(R_{g,ring}) \quad (6)$$

where x_{loop} is the primary loop fraction, $P(R_{g,bridge})$ is the form factor for a linear chain, and $P(R_{g,ring})$ is the form factor for a ring. Theoretical prestrain was calculated using a simplifying assumption previously invoked by Lin et al. whereby primary loops are Gaussian rings and all other strands in the network are bridging chains which do not change conformation upon gelation; this curve is therefore labeled "loops no stretch". Equation 6 was solved for the average predicted R_g (details in the Weighted Form Factor Analysis section in the SI), and the resulting prestrain estimate is plotted as a function of dimensionless concentration in Figure 4. Dimensionless concentration is used here because it enables a direct comparison across different chemical systems and molecular weights, which is challenging when working in traditional concentration or volume fraction units. Dimensionless concentration is defined as[50]

$$c_{dim} = cR^3 = c\langle R^2\rangle^{3/2} = cb^3\left(\frac{M}{m_0}\right)^{3/2} \quad (7)$$

where c is the molar polymer synthesis concentration and R denotes the root-mean-square end-to-end distance for the linear precursor, equivalent to $b\left(\frac{M}{m_0}\right)^{1/2}$, where M is the polymer molar mass and m_0 is the Kuhn segment molar mass. Figure 4 shows that the loops no stretch estimate agrees with high concentration poly(dimethylsiloxane) (PDMS) network prestrain measurements reported by Beltzung et al.,[32] but does not capture the prestrain data collected around the overlap concentration.

The measured prestrain clearly deviates from the loops no stretch estimate around the overlap concentration, suggesting that the elastically effective bridging strands must also deviate from their pregel conformations to offset the contraction of loops. Stretching of the bridging strands was estimated independently with both a form factor and volumetric scaling analysis. In the form factor analysis, the average R_g of a bridging strand was calculated with eq 6 using the average R_g extracted from the SANS data fitting to calculate $R_{g,bridge}$. Values of $R_{g,bridge}$ were calculated with both Debye and Guinier analyses, as detailed in the SI, and were then compared to the R_g of free chains in solution. The ratio $R_{g,bridge}/R_{g,solution}$ captures the effective stretching experienced by the linear bridging strands, which is plotted in Figure 5 and reported in Table S4. The extent of stretching ranged from 2−23% near the overlap concentration and increased as the synthesis concentration decreased.

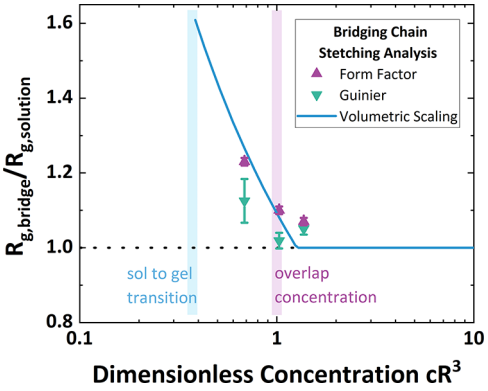

Figure 5. Ratio of the radius of gyration of bridging strands in a gel over the size in solution is plotted as a function of dimensionless concentration. The ratio was calculated with Debye form factor and Guinier analysis based on the SANS data and compared to a volumetric scaling analysis.

To independently estimate anticipated chain stretching, a scaling relationship was employed that relates the number of effective chains to the increase in radius the average chain would experience to fill a constant volume. The total volume, V_{tot}, scales as

$$V_{tot} \sim nV_{chain} \sim nr^3 \quad (8)$$

where n is the number of polymer molecules and V_{chain} is the volume each individual chain occupies, which scales as r^3. Since n is directly related to the concentration, changes in radius as the concentration falls below the overlap concentration should scale as

$$\left(\frac{n_{overlap}}{n_{bridge}}\right)^{1/3} = \left(\frac{r_{bridge}}{r_{overlap}}\right) \quad (9)$$

To account for topological defects in the gels, an effective elastic chain concentration of bridging molecules was calculated by subtracting the fraction of strands that are primary loops from the synthesis concentration; these adjusted chain concentrations are reported in the Chain Stretching Analysis section of the SI and are the basis for the calculation of r_{bridge}. Using eq 9 and $\phi_0^* \approx 0.057$ as the overlap concentration,[11,39] the percent change in r was calculated based on the concentration of bridging strands, reported as volumetric scaling in Table S2 and plotted as a function of dimensionless concentration in Figure 5.

Based on Figure 5 it is evident that the bridging polymer chains stretch by up to 25% when necessary to allow the cross-linking reaction to proceed to complete conversion. This stretching is well within the entropic regime for Gaussian chains, and there is precedent for stretching of much greater magnitude during gel swelling. In the case of prestrain,

https://doi.org/10.1021/acsmacrolett.3c00006
ACS Macro Lett. 2023, 12, 325−330

however, it is the kinetic process of network formation that drives chain extension. It should be stressed that while the prestrain measured here is an accurate reflection of the ensemble average of strands in the network, it does not differentiate between different populations of strand topologies.

In summary, prestrain was experimentally measured in dilute gels and found to increase as the concentration decreased, despite the increased prevalence of loop defects. Radii of gyration extracted from contrast matched SANS curves showed that single chains in the gel exhibit slightly larger conformations, on average, than single chains in solution. The extent of elastic strand stretching was quantitatively estimated to show that bridging strands will stretch up to 25% to create a space-spanning network around the overlap condition, emphasizing the need to consider individual strand behavior within a material. The measured prestrain provides a useful benchmark for theoretical calculations and future model refinement.

EXPERIMENTAL DETAILS

Hydrogenous and partially deuterated A_2 + B_4 PEG gels were synthesized over a range of concentrations (4−20 mM) following a previously published protocol.[20,25] Briefly, bifunctional linear PEG−OH (MW = 4600 g/mol, $Đ$ = 1.04, Sigma-Aldrich) and dPEG-OH (MW = 4800 g/mol, $Đ$ = 1.26, Creative PEGworks) were modified with azide-containing functional groups, dried, and brought into the glovebox to react with a tetra-functional alkyne cross-linker via copper-catalyzed alkyne azide click chemistry. Conversion reached >97% and >98% for the deuterated and hydrogenous coupling reactions, respectively (Figures S15−S17). Contrast matched gels were synthesized with 10% hydrogenous PEG and 90% deuterated PEG by molar ratio to match the scattering length density of the solvent, deuterated *N*,*N*-dimethylformamide. Synthesis and sample preparation details are included in the SI. Scattering length densities were calculated with the NIST web calculator;[51] densities and the resultant coherent and incoherent SLD's are found in Table S1. Small-angle neutron scattering was conducted at Oak Ridge National Laboratory Spallation Neutron Source and High Flux Isotope Reactor; SANS measurement details are included in the SI.

ASSOCIATED CONTENT

Supporting Information

The Supporting Information is available free of charge at https://pubs.acs.org/doi/10.1021/acsmacrolett.3c00006.

Contrast matching calculation; SANS sample preparation and experimental details; calculation of radius of gyration; uncertainty analysis; correlation length scaling; weighted form factor and chain stretching analysis; synthesis protocols, polymer GPC, and small molecule ^{1}H and ^{2}H NMR spectra (PDF)

AUTHOR INFORMATION

Corresponding Author

Bradley D. Olsen − *Department of Chemical Engineering, Massachusetts Institute of Technology, Cambridge, Massachusetts 02139, United States;* orcid.org/0000-0002-7272-7140; Email: bdolsen@mit.edu

Authors

Haley K. Beech − *Department of Chemical Engineering, Massachusetts Institute of Technology, Cambridge, Massachusetts 02139, United States;* orcid.org/0000-0003-3276-8578

Jeremiah A. Johnson − *Department of Chemistry, Massachusetts Institute of Technology, Cambridge, Massachusetts 02139, United States;* orcid.org/0000-0001-9157-6491

Complete contact information is available at: https://pubs.acs.org/10.1021/acsmacrolett.3c00006

Author Contributions

CRediT: **Haley K. Beech** conceptualization (supporting), data curation (lead), formal analysis (lead), investigation (lead), methodology (lead), writing-original draft (lead), writing-review & editing (equal); **Jeremiah A. Johnson** conceptualization (supporting), funding acquisition (supporting), project administration (supporting), resources (supporting), writing-review & editing (equal); **Bradley D. Olsen** conceptualization (lead), data curation (supporting), formal analysis (supporting), funding acquisition (lead), investigation (supporting), methodology (supporting), project administration (lead), resources (lead), writing-review & editing (equal).

Notes

The authors declare no competing financial interest.

ACKNOWLEDGMENTS

This work was supported by the NSF Center for the Chemistry of Molecularly Optimized Networks (MONET), CHE-2116298. We would like to acknowledge beamline scientists William Heller at SNS and Lilin He at HFIR for guidance in neutron data collection and reduction. We also acknowledge Charlotte Dai and Ameya Rao for assistance with neutron data collection.

REFERENCES

(1) James, H. M.; Guth, E. Statistical Thermodynamics of Rubber Elasticity. *J. Chem. Phys.* **1953**, *21* (6), 1039−1049.

(2) Flory, P. J. Network Structure and the Elastic Properties of Vulcanized Rubber. *Chem. Rev.* **1944**, *35* (1), 51−74.

(3) Flory, P. J. Molecular Theory of Rubber Elasticity. *Polymer* **1979**, *20*, 1317−1320.

(4) Neuss, S.; Blomenkamp, I.; Stainforth, R.; Boltersdorf, D.; Jansen, M.; Butz, N.; Perez-Bouza, A.; Knüchel, R. The Use of a Shape-Memory Poly(ε-Caprolactone)Dimethacrylate Network as a Tissue Engineering Scaffold. *Biomaterials* **2009**, *30* (9), 1697−1705.

(5) Langer, R.; Tirrell, D. A. Designing Materials for Biology and Medicine. *Nature* **2004**, *428*, 487−492.

(6) Hoare, T. R.; Kohane, D. S. Hydrogels in Drug Delivery: Progress and Challenges. *Polymer* **2008**, *49* (8), 1993−2007.

(7) Han, D. K.; Hubbell, J. A. Synthesis of Polymer Network Scaffolds from L-Lactide and Poly(Ethylene Glycol) and Their Interaction with Cells. *Macromolecules* **1997**, *30*, 6077−6083.

(8) Lange, F.; Schwenke, K.; Kurakazu, M.; Akagi, Y.; Chung, U.-I.; Lang, M.; Sommer, J.-U.; Sakai, T.; Saalwachter, K. Connectivity and Structural Defects in Model Hydrogels: A Combined Proton NMR and Monte Carlo Simulation Study. *Macromolecules* **2011**, *44*, 9666−9674.

(9) Zhou, H.; Woo, J.; Cok, A. M.; Wang, M.; Olsen, B. D.; Johnson, J. A. Counting Primary Loops in Polymer Gels. *Proc. Natl. Acad. Sci. U. S. A.* **2012**, *109* (47), 19119−19124.

(10) Zhou, H.; Schön, E.-M.; Wang, M.; Glassman, M. J.; Liu, J.; Zhong, M.; Díaz Díaz, D.; Olsen, B. D.; Johnson, J. A. Crossover Experiments Applied to Network Formation Reactions: Improved Strategies for Counting Elastically Inactive Molecular Defects in PEG Gels and Hyperbranched Polymers. *J. Am. Chem. Soc.* **2014**, *136*, 9464−9470.

(11) Zhong, M.; Wang, R.; Kawamoto, K.; Olsen, B. D.; Johnson, J. A. Quantifying the Impact of Molecular Defects on Polymer Network Elasticity. *Science* **2016**, *353* (6305), 1264−1268.
(12) Wang, J.; Lin, T.-S.; Gu, Y.; Wang, R.; Olsen, B. D.; Johnson, J. A. Counting Secondary Loops Is Required for Accurate Prediction of End-Linked Polymer Network Elasticity. *ACS Macro Lett.* **2018**, *7* (2), 244−249.
(13) Lin, T.-S.; Wang, R.; Johnson, J. A.; Olsen, B. D. Revisiting the Elasticity Theory for Real Gaussian Phantom Networks. *Macromolecules* **2019**, *52*, 1685−1694.
(14) Lang, M. Elasticity of Phantom Model Networks with Cyclic Defects. *ACS Macro Lett.* **2018**, *7*, 536−539.
(15) Lang, M. On the Elasticity of Polymer Model Networks Containing Finite Loops. *Macromolecules* **2019**, *52*, 6266−6273.
(16) Gusev, A. A. Numerical Estimates of the Topological Effects in the Elasticity of Gaussian Polymer Networks and Their Exact Theoretical Description. *Macromolecules* **2019**, *52*, 3244−3251.
(17) Tsimouri, I. C.; Schwarz, F.; Caseri, W.; Hine, P. J.; Gusev, A. A. Comparative Experimental and Molecular Simulation Study of the Entropic Viscoelasticity of End-Linked Polymer Networks. *Macromolecules* **2020**, *53* (13), 5371−5380.
(18) Rebello, N. J.; Beech, H. K.; Olsen, B. D. Adding the Effect of Topological Defects to the Flory-Rehner and Bray-Merrill Swelling Theories. *ACS Macro Lett.* **2021**, *10* (5), 531−537.
(19) Chassé, W.; Schlögl, S.; Riess, G.; Saalwächter, K. Inhomogeneities and Local Chain Stretching in Partially Swollen Networks. *Soft Matter* **2013**, *9* (29), 6943−6954.
(20) Arora, A.; Lin, T.-S.; Beech, H. K.; Mochigase, H.; Wang, R.; Olsen, B. D. Fracture of Polymer Networks Containing Topological Defects. *Macromolecules* **2020**, *53* (17), 7346−7355.
(21) Arora, A.; Lin, T.-S.; Olsen, B. D. Coarse-Grained Simulations for Fracture of Polymer Networks: Stress Versus Topological Inhomogeneities. *Macromolecules* **2022**, *55* (1), 4−14.
(22) Rubinstein, M.; Colby, R. H. *Polymer Physics*; Oxford University Press: New York, 2003.
(23) Panyukov, S. Theory of Flexible Polymer Networks: Elasticity and Heterogeneities. *Polymers* **2020**, *12* (4), 767.
(24) Flory, P. J. *Principles of Polymer Chemistry*; Cornell University Press: Ithaca, NY, U.S.A., 1953.
(25) Kawamoto, K.; Zhong, M.; Wang, R.; Olsen, B. D.; Johnson, J. A. Loops versus Branch Functionality in Model Click Hydrogels. *Macromolecules* **2015**, *48*, 8980−8988.
(26) Lang, M.; Sommer, J. U. Analysis of Entanglement Length and Segmental Order Parameter in Polymer Networks. *Phys. Rev. Lett.* **2010**, *104* (17), 2−5.
(27) Lang, M. Monomer Fluctuations and the Distribution of Residual Bond Orientations in Polymer Networks. *Macromolecules* **2013**, *46* (24), 9782−9797.
(28) King, J. S.; Boyer, W.; Wignall, G. D.; Ullman, R. Radii of Gyration and Screening Lengths of Polystyrene in Toluene as a Function of Concentration. *Macromolecules* **1985**, *18* (4), 709−718.
(29) Fetters, L. J.; Lohse, D. J.; Richter, D.; Witten, T. A.; Zirkel, A. Connection between Polymer Molecular Weight, Density, Chain Dimensions, and Melt Viscoelastic Proerpties. *Macromolecules* **1994**, *27* (17), 4639−4647.
(30) Benmouna, M.; Hammouda, B. The Zero Average Contrast Condition: Theoretical Predictions and Experimental Examples. *Prog. Polym. Sci.* **1997**, *22*, 49−92.
(31) Arrighi, V.; Higgins, J. S. Local Effects of Ring Topology Observed in Polymer Conformation and Dynamics by Neutron Scattering - A Review. *Polymers* **2020**, *12* (9), 1884.
(32) Beltzung, M.; Picot, C.; Rempp, P.; Herz, J. Investigation of the Conformation of Elastic Chains in Poly (Dimethylsiloxane) Networks by Small-Angle Neutron Scattering. *Macromolecules* **1982**, *15*, 1594−1600.
(33) Brás, A. R.; Pasquino, R.; Koukoulas, T.; Tsolou, G.; Holderer, O.; Radulescu, A.; Allgaier, J.; Mavrantzas, V. G.; Pyckhout-Hintzen, W.; Wischnewski, A.; Vlassopoulos, D.; Richter, D. Structure and Dynamics of Polymer Rings by Neutron Scattering: Breakdown of the Rouse Model. *Soft Matter* **2011**, *7* (23), 11169−11176.
(34) Brás, A. R.; Goosßen, S.; Krutyeva, M.; Radulescu, A.; Farago, B.; Allgaier, J.; Pyckhout-Hintzen, W.; Wischnewski, A.; Richter, D. Compact Structure and Non-Gaussian Dynamics of Ring Polymer Melts. *Soft Matter* **2014**, *10* (20), 3649−3655.
(35) Goosßen, S.; Brás, A. R.; Pyckhout-Hintzen, W.; Wischnewski, A.; Richter, D.; Rubinstein, M.; Roovers, J.; Lutz, P. J.; Jeong, Y.; Chang, T.; Vlassopoulos, D. Influence of the Solvent Quality on Ring Polymer Dimensions. *Macromolecules* **2015**, *48* (5), 1598−1605.
(36) Iwamoto, T.; Doi, Y.; Kinoshita, K.; Takano, A.; Takahashi, Y.; Kim, E.; Kim, T. H.; Takata, S. I.; Nagao, M.; Matsushita, Y. Conformations of Ring Polystyrenes in Semidilute Solutions and in Linear Polymer Matrices Studied by SANS. *Macromolecules* **2018**, *51* (17), 6836−6847.
(37) Iwamoto, T.; Doi, Y.; Kinoshita, K.; Ohta, Y.; Takano, A.; Takahashi, Y.; Nagao, M.; Matsushita, Y. Conformations of Ring Polystyrenes in Bulk Studied by SANS. *Macromolecules* **2018**, *51* (4), 1539−1548.
(38) Ying, Q.; Chu, B. Overlap Concentration of Macromolecules in Solution. *Macromolecules* **1987**, *20* (2), 362−366.
(39) Akagi, Y.; Gong, J. P.; Chung, U. Il; Sakai, T. Transition between Phantom and Affine Network Model Observed in Polymer Gels with Controlled Network Structure. *Macromolecules* **2013**, *46* (3), 1035−1040.
(40) Roe, R.-J. *Methods of X-ray and Neutron Scattering in Polymer Science*; Oxford University Press: New York, 2000.
(41) Ornstein, L. S.; Zernike, F. Accidental Deviations of Density and Opalescence at the Critical Point of a Single Substance. *Proc. Akad. Sci.* **1914**, *17* (2), 793−806.
(42) Matsunaga, T.; Sakai, T.; Akagi, Y.; Chung, U. Il; Shibayama, M. Structure Characterization of Tetra-PEG Gel by Small-Angle Neutron Scattering. *Macromolecules* **2009**, *42* (4), 1344−1351.
(43) Sakai, T.; Matsunaga, T.; Yamamoto, Y.; Ito, C.; Yoshida, R.; Suzuki, S.; Sasaki, N.; Shibayama, M.; Chung, U. Il. Design and Fabrication of a High-Strength Hydrogel with Ideally Homogeneous Network Structure from Tetrahedron-like Macromonomers. *Macromolecules* **2008**, *41* (14), 5379−5384.
(44) Matsunaga, T.; Sakai, T.; Akagi, Y.; Chung, U. Il; Shibayama, M. SANS and SLS Studies on Tetra-Arm PEG Gels in as-Prepared and Swollen States. *Macromolecules* **2009**, *42* (16), 6245−6252.
(45) Akagi, Y.; Matsunaga, T.; Shibayama, M.; Chung, U. Il; Sakai, T. Evaluation of Topological Defects in Tetra-PEG Gels. *Macromolecules* **2010**, *43* (1), 488−493.
(46) Matsunaga, T.; Asai, H.; Akagi, Y.; Sakai, T.; Chung, U. Il; Shibayama, M. SANS Studies on Tetra-PEG Gel under Uniaxial Deformation. *Macromolecules* **2011**, *44* (5), 1203−1210.
(47) Akagi, Y.; Sakurai, H.; Gong, J. P.; Chung, U. Il; Sakai, T. Fracture Energy of Polymer Gels with Controlled Network Structures. *J. Chem. Phys.* **2013**, *139* (14), 144905.
(48) Asai, M.; Katashima, T.; Chung, U. Il; Sakai, T.; Shibayama, M. Correlation between Local and Global Inhomogeneities of Chemical Gels. *Macromolecules* **2013**, *46* (24), 9772−9781.
(49) Yao, H.; Olsen, B. D. SANS Quantification of Bound Water in Water-Soluble Polymers across Multiple Concentration Regimes. *Soft Matter* **2021**, *17* (21), 5303−5318.
(50) Wang, R.; Alexander-Katz, A.; Johnson, J. A.; Olsen, B. D. Universal Cyclic Topology in Polymer Networks. *Phys. Rev. Lett.* **2016**, *116* (18), 1−5.
(51) Kienzle, P. Neutron activation and scattering calculator. https://www.ncnr.nist.gov/resources/activation/.

https://doi.org/10.1021/acsmacrolett.3c00006
ACS Macro Lett. 2023, 12, 325−330